DEVELOPMENT OF TUNGSTEN BASED ALLOY THROUGH NANO STRUCTURING

THESIS SUBMITTED IN PARTIAL FULFILLMENT OF THE REQUIREMENTS FOR THE DEGREE

OF

BECHLORE OF TECHNOLOGY

IN

METALLURGICAL AND MATERIALS ENGINEERING

BY

SASWAT KUMAR BEHERA (110MMM0485)

AND

SONU KUMAR PRAJAPATI (111MM0574)

UNDER THE GUIDENCE OF

PROF. ANSHUMAN PATRA

Department of Metallurgical and Materials Engineering
NIT Rourkela, Odisha.
May, 2015

CERTIFICATE

This is to certify that the thesis entitled ***'DEVLOPMENT OF TUNGSTEN BASED ALLOY USING NANO-STRUCTURING' submitted by SASWAT KUMAR BEHERA (110MM0485)*** *and* ***SONU KUMAR PRAJAPATI (111MM0574)*** *in partial fulfilment of the requirements for the award of* ***BACHELOR OF TECHNOLOGY*** *degree in* ***METALLURGICAL AND MATERIALS ENGINEERING*** *at the* ***NATIONAL INSTITUTE OF TECHNOLOGY, ROURKELA,*** *during the academic session 2014-2015 is an original work carried out by them under my supervision and guidance.*

The matter embodied in the thesis has not been submitted to any other University/institute for the award of any degree or diploma.

DATE-6th May, 2015

PROF.ANSHUMAN PATRA

DEPARTMENT OF METALLURGICAL AND MATERIALS ENGINEERING

NATIONAL INSTITUTE OF TECHNOLOGY, ROURKELA: 769008

ACKNOWLEDGMENT

We would like to express our sincere gratitude to ***Prof. S.C MISHRA****, Head of the Department, Metallurgical and Materials Engineering, NIT Rourkela for giving us an opportunity to work on this project and provide the valuable resources of the department.*

With great pleasure, we would like to express our deep sense of gratitude and ineptness to our guide, ***Prof. ANSHUMAN PATRA*** *Department of Metallurgical and Materials Engineering, NIT Rourkela, for his valuable guidance, constant encouragement and kind help throughout the project work and the execution of the dissertation work.*

We would also like to extend our sincere thanks to ***Prof. UDAY KUMAR SAHU*** *Department of Metallurgical and Materials Engineering, NIT Rourkela, for providing valuable insight and assistance during the experimental work.*

Finally, I am greatly indebted to my dear friends, family and soul whose support will always be remembered. They supported my endeavour for knowledge and my passion for learning owes to their encouragement.

Date-6th May, 2015

SASWAT KUMAR BEHERA

(110MM0485)

SONU KUMAR PRAJAPATI

(111MM0574)

ABSTRACT

Tungsten based alloys are extensively used in the defence application due to their high density and ability to withstand very high temperature. Solid state processing of pure W and W based alloys is, however, a difficult task due to the high sintering temperature (2700°C) required to sinter them. Liquid phase sintered W heavy alloys has been used as penetrators, but they can't be used for applications above 1200°C. Recently has shown that the sintering temperature of pure W could be brought down to ~1800°C from the conventional 2700°C by making the W-powder nanostructured prior to sintering. Present work aims at developing oxidation resistant W-based refractory alloys through mechanical alloying is followed by solid state sintering at modest temperature. Proper sintered alloys has to be studied.

Sintered density of $W_{50}Mo_{50}$ after sintering for 300 min at 1500°C was 92.5%, and it could be considered as a very significant extent of densification at this relatively low temperature, when compared to conventional sintering of microcrystalline W at 2700°C or above. Mechanical properties viz., hardness and elastic modulus of sintered W, determined by Nanoindentation tests, have been nearly similar to that of the conventional sintered W.

The crystallite size and lattice strain of the nanostructured powders have been calculated from the X -ray diffraction patterns by Williamson-Hall method. Results of analysis showed that crystallite size of elemental W powder could be brought down to 40 nm after five h of ball milling. But further milling caused a significant level of contamination from the grinding media indicating severe work hardening of nanostructured W.

CONTENTS

……@@###@@……

List of Figures with Captions

INTRODUCTION

1.1 BACKGROUND

The term Nano is fundamentally spoken to the one billionth of a meter. Along these lines, at whatever point we consider Nanoscience or nanotechnology it suggests little protests that ring a bell. In reality, this branch of science and innovation manages materials having no less than one spatial measurement in the size scope of 1 to 100 nm.

Richard P. Feynman (Nobel Laureate in Physics, 1965) is frequently credited for presenting the idea of nanotechnology. In the yearly meeting of the American Physical Society at California Institute of Technology on 26 December 1959, he conveyed a popular address entitled "There's Plenty of Room at the Bottom". In this address, he discussed written work twenty-four volumes of the Encyclopedia Britannica on the leader of a pin, and miniaturizing the PC (Feynman, 1992). He additionally proposed that it would be conceivable to organize the particles the way we need. In this way, a physicist ought to have the capacity to incorporate any compound substance by putting the molecules down where the scientist says. Tungsten combinations have been utilized as a part of different applications. The conventional fabrication procedure of tungsten composite included fluid stage sintering. Mechanical properties of tungsten combinations have been known to be enhanced by the refinement of microstructures by mechanical alloying which was an advantageous strong state union substitute to liquefy turning and comparable quick quenching techniques to create indistinct amalgams. High-Energy ball milling has picked up very ubiquity as of late on account of its straightforwardness, simplicity scale up creation, high profitability, moderately cheap hardware, and relevance to a broad mixture of materials. Mechanical alloying (MA) has now been demonstrated to be fit for combining an assortment of balance and non-harmony combination stages beginning from mixed essential or prealloyed powders. The non-harmony stages synthesized incorporate supersaturated strong arrangements, metastable crystalline and quasicrystalline stages, nanostructures, and nebulous composites [1, 2].

1.2 CONVENTIONAL PROCESSING

Tungsten can be used as a high-temperature structural material because of its excellent properties, such as high melting point of 3410°C, density of 19.3 g/ml, hardness of 9.8 GPa, elastic modulus of 411 GPa, low co-efficient of thermal expansion, high thermal conductivity

[3, 4].Moreover at a conventional sintering temperature of more than 2700°C deteriorated the mechanical properties of sintered tungsten components [5-7].

1.3 IMPORTANCE OF NANO STRUCTURE FORMATION

Decrease in crystal size there is decrease in the melting temperature as well the sintering temperature [8].Thermodynamically Nanopowders are unstable due to large surface area. Nanoparticles acquire different surface energies than usual ones. Kinetically, sintering of Nanopowders are significantly enhanced. Hence, sintering of nanopowders of tungsten based alloys indicated depressed sintering onset temperatures as compared to conventional powders. The Lower sintering temperature is beneficial for many reasons such as the elimination of sintering aids, avoiding undesirable phase transformation, and deleterious decomposition or interfacial reactions. The ability to sinter W based alloys at reduced temperature would make the fabrication of high-temperature structural components easier.

1.4 OBJECTIVE OF PRESENT STUDY

Tungsten based alloy are very useful because of their wide range of properties. The mechanically Milled nanocrystalline powder of tungsten has restricted the grain growth and showed improved mechanical properties of the sintered product compared to other. The oxidation resistance of the sintered alloys has to be studied for high-temperature applications. Oxidation resistance has been obtained either by alloying or by providing viscous slag.

LITERATURE REVIEW

2.1 TUNGSTEN BASED ALLOYS

Tungsten is the refractory metal that possess high melting point (3410°C) and excellent mechanical strength at elevated temperature and the highest density (19.3 g/ml) and tensile elastic modulus (411 GPa at 20°C) of all engineering materials [3 ,4]. Tungsten forms volatile oxides at elevated temperatures, thus severely limiting their usefulness in oxidizing environments.Tungsten based alloys are known as heavy alloys (WHA) are the materials of choice for tungsten based penetrators. Tungsten alloys have been used in various applications such as industrial and military applications such as balance weights in airplanes, radiation shields, missile warhead prefragments, and kinetic energy penetrators.

2.2 MECHANICAL ALLOYING

Mechanical alloying (MA) is a powder processing technique that allows the production of homogeneous materials starting from blended elemental powder mixtures. Mechanical alloying is normally a dry, high-energy ball milling technique and has been employed to produce a variety of commercially useful and scientifically interesting materials. Additionally, it has been recognized that powder mixtures can be mechanically activated to induce chemical reactions, i.e., mechanochemical reactions at room temperature or at least at much lower temperatures than normally required to produce pure metals, nanocomposites, and a variety of commercially useful materials. The non-equilibrium phases that are being synthesized include supersaturated solid solutions, metastable crystalline and quasicrystalline phases, nanostructures and amorphous alloys.

2.2.1 PROCESS OF MECHANICAL ALLOYING

The actual process of MA starts with mixing of the powders in the right proportion and loading the powder mix into the mill along with the grinding medium (generally steel balls). This mix is then milled for the desired length of time until a steady state is reached when the composition of every powder particle is the same as the proportion of the elements in the starting powder mix. The milled powder is then consolidated into a bulk shape and heat treated to obtain the desired microstructure and properties. Thus the essential components of the MA process are the raw materials, the mill, and the process variables. We will now discuss the deferent parameters involved in the selection of raw materials, types of mills, and process variables.

Koch [9] has presented the work of Fecht who has summarized a three-stage mechanism for the development of nanocrystalline material by mechanical alloying/milling as below:

Stage 1: Deformation localization in shear bands containing a high dislocation density.

Stage 2: Dislocation annihilation/recombination/rearrangement to form a cell/subgrain Structure with nanoscale dimensions-further milling extends this structure throughout the sample.

Stage 3: The orientation of the grains becomes random, i.e. low angle grain boundaries develop to high angle grain boundaries introduction of defects, grain boundary sliding, grain rotation, etc.

During high energy milling the powder particles are repeatedly flattened, cold welded, fractured and rewelded [1, 2]. Whenever two steel balls collide, some amount of powder is trapped in between them. Typically, around 1000 particles with an aggregate weight of about 0.2 mg are trapped during each collision. The force of the impact plastically deforms the powder particles leading to work hardening and fracture. The new surfaces created enable the particle to weld together, and this leads to increase in particle size.

A broad range of particle sizes develops with some as large as three times bigger than the starting particles. The composite particles at this stage have a characteristic layered structure consisting of various combinations of the starting constituents. With continued deformation, the particles get work hardened and fracture by a fatigue failure mechanism and/or by the fragmentation of fragile flakes [1, 2]. Fragments generated by this mechanism may continue to reduce in size in the absence of strong agglomerating forces. At this stage the tendency to fracture predominates over cold welding. Due to the continued impact of the grinding balls, the structure of the particles is steadily refined, but the particle size continues to be the same. Consequently the inter-layer spacing decreases and the number of layers in a particle increase. However the efficiency of particle size reduction is very low, about 0.1% in a conventional ball mill. The efficiency may be somewhat higher in higher energy ball milling processes, but it is still less than 1%. The remaining energy is lost mostly in the form of heat, but a small amount is also utilized in the elastic and plastic deformation of the powder particles [1, 2]. After milling for a certain length of time, steady-state equilibrium is attained when a balance is achieved between rate of welding, which tend to increase the average particle size, and the rate of fracturing, which tends to decrease the average composite particle size.

2.2.1.1 RAW MATERIAL

The raw materials used for MA are widely available commercially pure powders that have particle sizes in the range of 1-200 μm. But, the powder particle size is not very critical, except that it should be smaller than the grinding ball size. This is because the powder particle size decreases exponentially with time and reaches a small value of a few microns only after a few minutes of milling. The raw powders fall into the broad categories of pure metals, master alloys, pre alloyed powders, and refractory compounds. Metal powders are sometimes milled with a liquid medium and this is referred to as wet grinding, if no liquid is involved then it is referred to as dry grinding. Cryomilling also is wet grinding, if the liquid

used is at cryogenic temperature). It has been reported that wet grinding is a more suitable method than dry grinding to obtain finer-ground products because the solvent molecules are adsorbed on the newly formed surfaces of the particles and lower their surface energy. The less- agglomerated condition of the powder particles in the wet condition is also a useful factor and it helps in compaction and sintering.

2.2.1.2 TYPES OF MILLS

Different types of high-energy milling equipment are used to produce mechanically alloyed powders. They differ in their capacity, the efficiency of milling and additional arrangements for cooling, heating, etc. Depending on the type of powder, the quantity of the powder, and the final constitution required, a suitable mill can be chosen.

(A) HIGH ENERGY SHAKER MILL

The amplitude (about 5 cm) and speed (about 1200 rpm) of the clamp motion, the ball velocities are high (on the order of 5 m/s) and consequently the force of the ball's impact is unusually great. Therefore, these mills can be considered as high-energy variety.

(B) PLANETARY BALL MILL

Another popular mill for conducting MA experiments is the planetary ball mill (referred to as Pulverisette) in which a few hundred grams of the powder can be milled at a time. These are manufactured by Fritsch GmbH in Germany and marketed by Gilson Co., in the US and Canada. The planetary ball mill owes its name to the planet-like movement of its vials. These are arranged on a rotating support disk and a special drive mechanism causes them to rotate around their own axes. The centrifugal force produced by the vials rotating around their own axes and that produced by the rotating support disk both act on the vial contents, consisting of material to be ground and the grinding balls. Since the vials and the supporting disk rotate in opposite directions, the centrifugal forces alternately act in like and opposite directions.

(C) ATTRITOR MILL

An attritor (a ball mill capable of generating higher energies) involves of a vertical drum with a series of impellers inside it. Attritors of different sizes and capacities are available. The grinding tanks or containers are available either in stainless steel or stainless steel coated

inside with alumina, silicon carbide, silicon nitride, zirconia, rubber, and polyurethane. A variety of grinding media also is available as glass, steatite ceramic, mullite, silicon carbide, silicon nitride, sialon, alumina, zirconium silicate, zirconia, stainless steel, carbon steel, chome steel, and tungsten carbide. The operation of an attritor is simple. The powder to be milled is placed in a stationary tank with the grinding media. This mixture is then agitated by a shaft with arms, rotating at a high speed of about 250 rpm. This causes the media to exert both shearing and impact forces on the material. The laboratory attritor works up to 10 times faster than conventional ball mills.

(D) COMMERCIAL MILLS

Commercial ball mills used for MA are much larger in size than the mills described above and can process several hundred pounds at a time. Mechanical alloying for commercial production is carried out in ball mills of upto about 3000 lb (1250 kg) capacity.

(E) NEW DESIGNS

Several new designs of mills have been developed in recent years for specialized purposes. These include the rod mills, vibrating frame mills, and the equipment available from Dymatron, Cincinnati, OH; Super Misuni NEV-MA-8 from Nisshin Giken, Tokyo, Japan Uni-Ball-Mill from Australian Scientific Instruments, Canberra, Australia, HEMill from M.B.N. srl, Rome, Italy; and Zoz Maschinenbau GmbH, Kreuztal, Germany.

2.2.1.3 PROCESS VARIABLES

Mechanical alloying is a complex process and hence involves optimization of a number of variables to achieve the desired product phase and/or microstructure. Some of the important parameters that have an effect on the final constitution of the powder are as follows [1, 2],

- Type of mill,
- Milling Container,
- Milling Speed,
- Milling Time,
- Type, Size and Size distribution of grinding medium,
- Ball-to-powder weight ratio,
- Extend of filling the vial,

- Wet or dry milling,
- Milling atmosphere,
- Process control agent, and
- Temperature of milling.

2.3 CONSOLIDATION OF NANOCRYSTALLINE POWDER

Groza [10] has reported that powder agglomeration, high reactivity, contamination, grain coarsening are the main problem of nanocrystalline powder consolidation. Low temperatures for minimizing grain growth may hinder good intergranular bonding thus providing the expected high mechanical strength and ductility. This has been accomplished by major development in nanopowder synthesis techniques and understanding the effect of porosity.
Some reports in tungsten powder consolidation some earlier reports [11] show that the products often have the same property as attained with traditional powders. At a conventional compaction pressure many nanoscale tungsten based alloys have insufficient green strength for handling. Binders could be used to increase green strength, but contamination arises since the small powder reacts with the binder during heating. Alternatively high compaction pressure without and added binders can be a potential route with less contamination.

2.4 NANOSINTERING OF TUNGSTEN BASED ALLOYS

Tungsten is traditionally sintered at a temperature above 2700□C under hydrogen atmosphere using high-temperature furnaces. Tungsten heavy alloys (less than 85% W) are compacted and solid state sintered form elemental powders whereas alloys containing greater than 85% W are liquid phase sintered to high densities. Such solid state sintered low W alloys having high ductility and strength consistently. For these reasons solid state sintering of full range of tungsten alloys to full, 100% densities is of interest. The processes are extremely expensive and also at elevated temperature grain growth of tungsten deteriorates the mechanical properties of sintered product. Thermodynamically nanopowders are unstable due to large surface area. Nanoparticles adopt different surface energies than regular ones, for instance by a different local atomic arrangement at the surface. Therefore sintering of nanopowders of tungsten and tungsten based alloys have designated depressed sintering onset temperatures as compared to conventional powders. The lower sintering temperature is

beneficial in different ways such as the elimination of sintering aids, avoiding undesirable phase transformation, and deleterious decomposition or interfacial reactions.

2.5 NANOCRYSTALLINE MATERIALS

Nanocrystalline materials are structurally characterized by a large volume fraction of grain boundaries, which may significantly alter a variety of physical, mechanical, and chemical properties with respect to the conventional coarse-grained (>1mm or even micron-size grains) polycrystalline materials. Nanocrystalline materials provide us not only with an excellent opportunity to study the nature of solid interfaces and to extend our understanding of the structure-property relationship in solid materials down to the nanometer regime, but also present an attractive potential for technological applications with their novel properties. Nanocrystalline materials have been synthesized by a number of techniques starting from the vapor phase (e.g., inert gas condensation) [12, 13], liquid phase (e.g., electrodeposition, rapid solidification), and solid state (e.g., mechanical attrition) [1-2]. The advantage of using MA for the synthesis of nanocrystalline materials lies in its ability to produce bulk quantities of material in the solid state using simple equipment and at room temperature.

2.5.1 CLASSIFICATION OF NANOCRYSTALLINE MATERIALS

Nanocrystalline materials can be classified into different categories depending on the number of dimensions in which the material has nanometer modulations. Thus, they can be classified into (a) layered or lamellar structures, (b) filamentary structures, and (c) equiaxed nanostructured materials. A layered or lamellar structure is a one dimensional (1D) nanostructure in which the magnitudes of length and width are much greater than the thickness that is only a few nanometers in size. A two-dimensional (2D) rod-shaped nanostructure can be termed filamentary and in this the length is substantially larger than width or diameter, which are of nanometer dimensions. The most common of the nanostructures, is basically equiaxed (all the three dimensions are of nanometer size) and are termed nanostructured crystallites [thee- dimensional (3D) nanostructures], zero dimensional clusters are also considered elsewhere. The nanostructured materials may contain crystalline, quasicrystalline, or amorphous phases and can be metals, ceramics, polymers, or composites. If the grains are made up of crystals, the material is called nanocrystalline. On the other hand, if they are made up of quasicrystalline or amorphous (glassy) phases, they are termed nanoquasicrystals and nanoglasses, respectively [14].

2.5.2 SYNTHESIS OF NANOCRYSTALLINE MATERIALS

Nanocrystalline materials can be synthesized either by consolidating small clusters or breaking down the bulk material into smaller and smaller dimensions. Gleiter [12, 13] used the inert gas condensation technique to produce nanocrystalline powder particles and consolidated them in situ into small disks under ultra-high vacuum (UHV) conditions. Since then a number of techniques have been developed to prepare nanostructured materials starting from the vapor, liquid, or solid states. Nanostructured materials have been synthesized in recent years by methods including inert gas condensation, mechanical alloying, spray conversion processing, severe plastic deformation, electro deposition, rapid solidification from the melt, physical vapor deposition, chemical vapor processing, co-precipitation, sol-gel processing, sliding wear, spark erosion, plasma processing, laser ablation, quenching the melt under high pressure of amorphous phases. Actually, in practice any method capable of producing very fine grain-sized materials can be used to synthesize nanocrystalline materials. The grain size, morphology, and texture can be varied by suitably modifying/controlling the process variables in these methods. The choice of the method depends upon the ability to control the most important feature of the nanocrystalline materials, viz., the microstructural features (grain size, layer spacing, etc.).

2.5.3 OXIDATION OF TUNGSTEN BASED ALLLOYS

Tungsten has high melting point and very good mechanical strength at high temperature, but tungsten oxidizes very quickly at moderate temperature so many limitation is there in the use at open environment. The oxidation reaction was found to follow the parabolic rate law initially but transformed to a linear rate law for thick films. Three stages are recognized in oxidation of W based alloys: an incipient, "transient stage characterized by simultaneous formation of oxides of every active component; a "steady state" stage coinciding with the development of protective film and governed by the continued growth of the continuous layer; and finally accelerated attack or "breakaway" stage.

Tungsten possesses high melting point and excellent mechanical strength at elevated temperature, but tungsten oxidizes very rapidly at even moderate temperature thus severely limiting their usefulness in oxidizing environment. Wysong [15] has reported that oxidation of tungsten follows the parabolic rate law between 400° to 500°C. Webb, Norton, and Wagner [16] has studied the oxidation of tungsten between 700° to 1000°C. The oxidation reaction has been found to follow the parabolic rate law initially but transformed to a linear

rate law for thick films. Semmel [17] has reported that oxidation of tungsten changes from linear to parabolic rate law as the temperature was increased. Oxide melting was proposed to account for the decrease in the oxidation rate above 1150°C.

EXPERIMENTAL

3.1 SYNTHESIS OF NANOSTRUCTURED POWDERS

Elemental powders of W, Mo,(purity 99.5%,) with initial particle of 100-150 µm (for W, Mo) have been subjected to mechanical alloying at a mill speed of 300 r.p.m using chome steel as grinding media, toluene as a process control agent. Ball to powder weight ratio of 10:1 has to be maintained. Milled samples have been taken out after 1, 5, 10, 15, 20 h for the characterization purpose. A high resolution x- ray diffractometer (λ=1.541874 Å) has been used to record the X-ray diffraction pattern (XRD) of the mechanically alloyed powders at different stages of milling. The crystal size and lattice strain has been evaluated by determining the peak position and broadening of the peak from the X- ray diffraction pattern [18]. The lattice parameter by using precise lattice parameter calculation method [19]. The dislocation density of the milled powders was calculated as below:

$$\rho_d = 2\sqrt{3}\frac{\sqrt{\varepsilon^{1/2}}}{D\ X\ b} \qquad (1)$$

Where, b represent the burgers vector of dislocations, b = (a√3)/2 for the bcc structure, a= cell parameter= lattice parameter, D represent the crystallite size, ε represent the lattice strain [20-22].

The powders milled for 20 h were subjected to compaction in a uniaxial press 500 MPa 700 MPa 1000 MPa for 5 minutes. Sintering of the compacted pellets was carried out in a tunnel type sintering furnace at 1500°C for 2 h by purging argon into the furnace at a rate of 100 ml/min. Densities of the sintered products were evaluated by Archimedes's principle as below [23-25]:

$$\rho_s = \frac{W_a}{(W_{sat} - W_{susp})}\ X\ \rho_w \frac{gm}{cm^3} \qquad (2)$$

Where W_a is weight of the sintered sample in air. W_{sat} is the weight of the sample with all the open porosity saturated with water, W_{susp} is the weight suspended in water. ρ_w is the density of water.

The compression test was carried out to determine the maximum compressive strength of the sintered samples. The load and time and sliding speed during wear test was kept at 20 KN and 10 mins and 25 rpm respectively. The wear test is done to get the wear resistance of any material under cyclic loading with reference to time. The oxidation study of sintered sample is done at 1000°C for 6 h in a raising hearth furnace. The weight of the samples were measured using a microbalance. The rate of oxidation has been reported as weight change per unit area.

Table.1: Compositions of alloys chosen and ball milling details

Alloy	Composition Wt. %	Grinding Medium	Ball Size (mm)	Ball to powder weight ratio	Mill speed (rpm)	Milling Duration (h)	Medium
A	$W_{90}Mo_{10}$	Chome Steel	10	10:1	300	20	Toluene
B	$W_{70}Mo_{30}$	Chome Steel	10	10:1	300	20	Toluene
C	$W_{50}Mo_{50}$	Chome Steel	10	10:1	300	20	Toluene

RESULT AND DISCUSSION

4.1 XRD ANALYSIS

Fig. 1 displays the XRD patterns of all alloy powder subjected to milling at 0 to 20 h. Fig. 1(a) shows the XRD pattern of alloy A indicates that Mo undergoes into complete solid solution in W matrix. Refinement of crystallite size of W is evident from continuous

broadening and reduction in intensity of 5 to 20 h milled samples. A similar trend has also found in alloys B through C (Fig. 1(b) to (c)).

Variation of crystallite size and lattice strain for all the alloys is shown in Fig.2 (a) and Fig. 2 (b). Reduction in crystallite size and plastic strain build-up is attributed to the increase in full-width at half-maximum with increasing milling time. It is evident from Fig. 2 (a) that crystallite size is minimum for alloy C ($W_{50}Mo_{50}$) than the rest of the alloys. This is due to high surface energy provided by the high percentage of molybdenum particle.

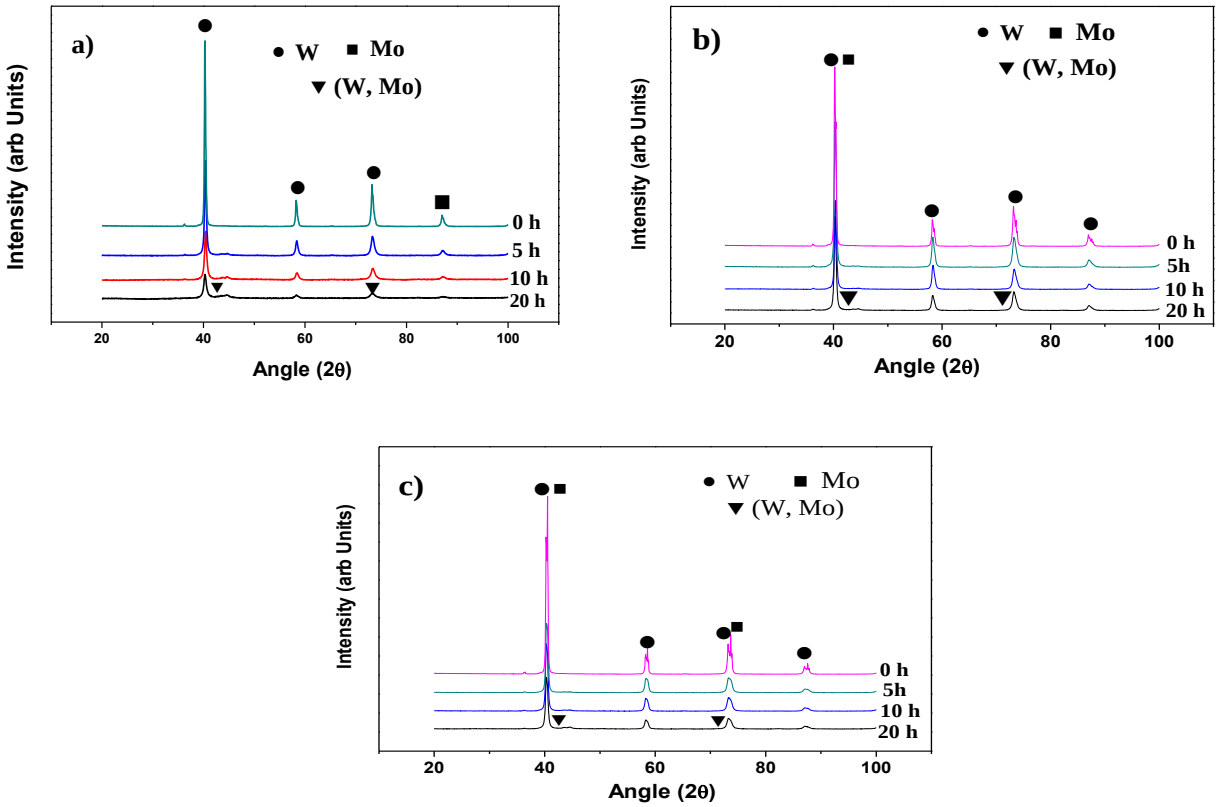

Fig.1. XRD pattern of powder milled for different times (0, 5, 10, 20 h) (a) $W_{90}Mo_{10}$, (b) $W_{70}Mo_{30}$, (c) $W_{50}Mo_{50}$.

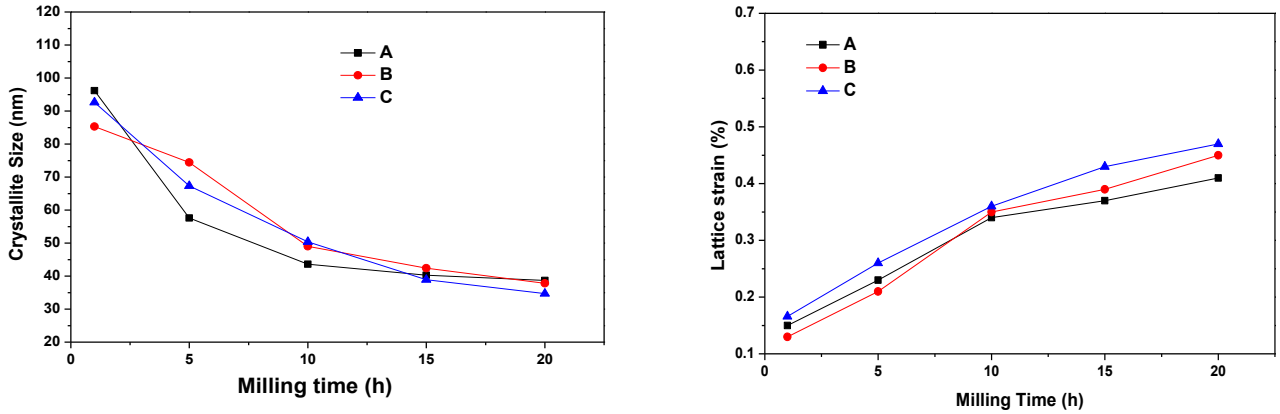

Fig. 2. (a) Variation of Crystallite size and (b) lattice strain with milling time of alloys A through C.

It is evident from Fig. 2 (a) that crystallite size is minimum for the alloy ($W_{50}Mo_{50}$) than the rest of the alloys. This is due to high surface energy provided by the high percentage of molybdenum particle. The dislocation density induced in all as milled powder (A through C) shows sharp increase with increase in grinding time to 10 h whereas moderate increase is evident beyond 10 to 20 h of milling (Fig 3 (a)). This attributed to predominant crystallite size reduction and rapid increase in the lattice strain during the period of 10 h of milling. Beyond 10 h of milling, the formation of solid solution (alloying Mo with W) is dominant over deformation of powder particles which leads to the reduction in the rate of increase of dislocation density.

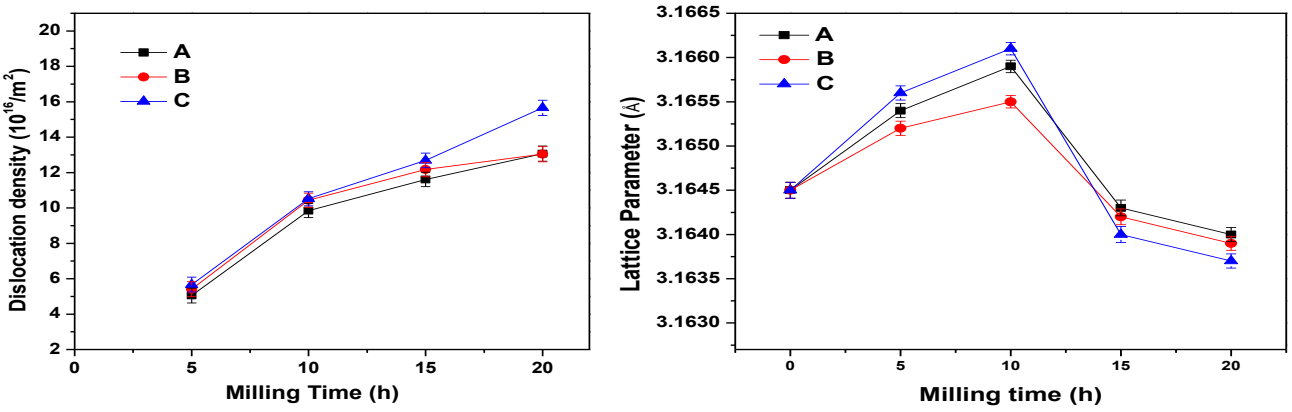

Fig. 3. (a) Variation of dislocation density with milling time and (b) Variation of Lattice parameter with milling time of alloys A through C respectively.

Fig. 3(b) represents that the lattice parameter of W in all alloys (A through C) initially increases at ten h of milling. This is attributed to the negative hydrostatic pressure applied due to the formation of nano-crystallites during mechanical alloying. Contraction of W lattice in all alloys (A through C) occurs at 20 h of milling. This is due to the formation of a

substitutional solid solution by Mo with W. Fig. 4 shows the XRD pattern of all sintered alloys (A through C). Formation of any deleterious phase transformations or any unwanted phase which may cause a severe negative impact on the mechanical properties of the alloys are not evident from XRD pattern.

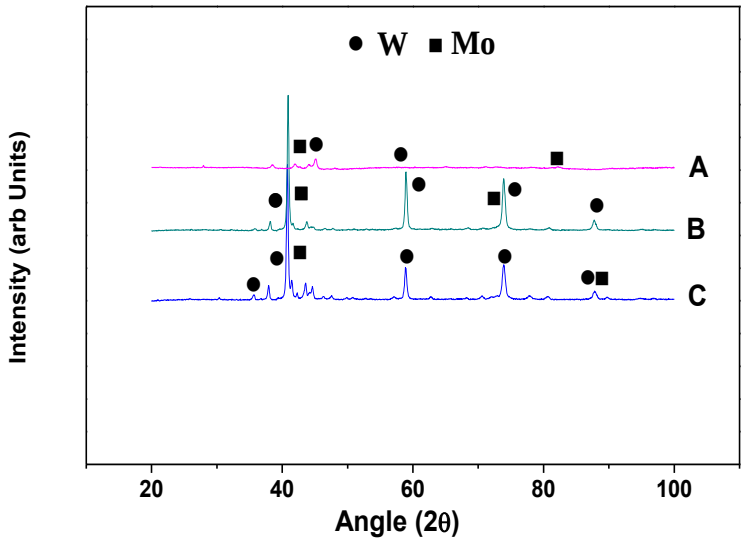

Fig 4. XRD pattern for alloys A through C milled for 20h and sintered at 1500°C for 2 h.

4.2 SEM ANALYSIS

Fig. 5.1 (a-d) shows the variation in particle size and morphology as evident from SEM images with increase in milling time from 0 to 20 h for alloy A. as we can see that initially the decrease in size up to the 10 h is very high (Fig. 5.1c), and after the 10h till 20 h the size reduction is not much high, this is because initially due to negative hydrostatic pressure by nano- crystals, after 10 h due to formation of solid solution the rate of crystallite size reduction decreases. The homogenous of the particle also depends upon the milling time as milling time increases the homogeneity of the particle increases because of the smaller and similar size of the milled powder particles.

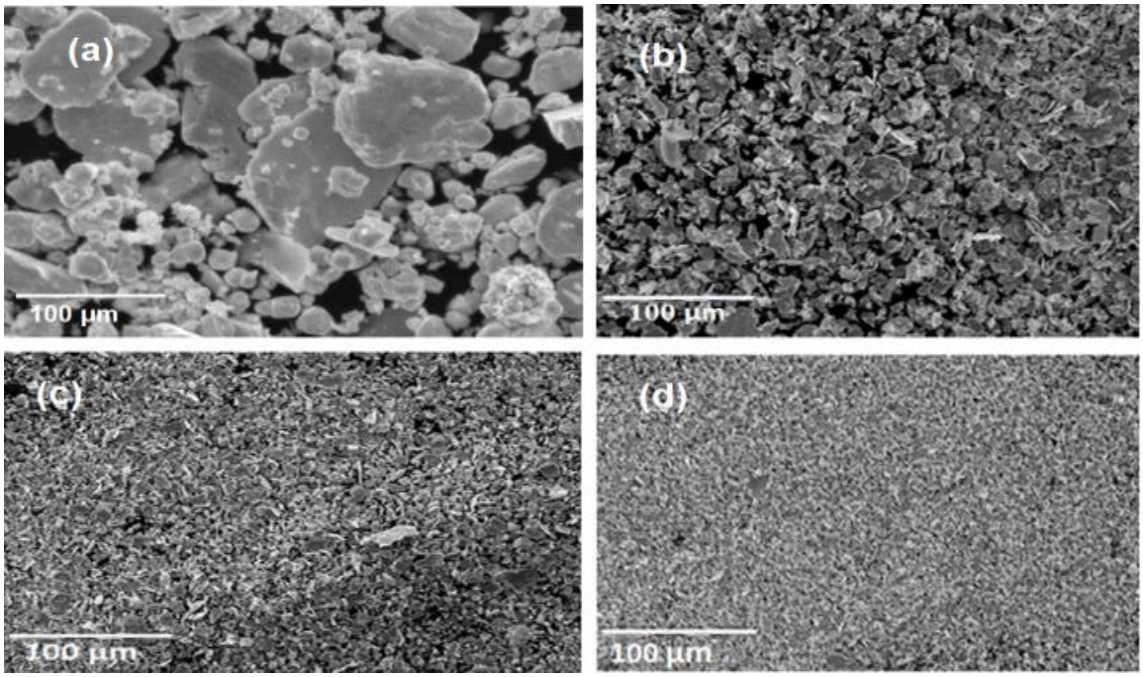

Fig. 5.1 SEM micrograph of powder morphology of alloy A after different milling times: (a) 0 h, (b) 5 h, (c) 10 h, and (d) 20 h.

It is evident from the SEM result that particle size reduces from micron level to sub-micrometer level with more homogeneous distribution and more amount of solute (i.e. molybdenum) moves into the solid solution with the increase in milling time as shown in XRD pattern (Fig. 1(a)). The SEM micrographs of alloys A to C sintered at 1500°C are shown in Fig. 5.2. Fig.5.2 (a) shows the micrograph of alloy A which indicates the presence of the dark phase (Mo) distributed in the W matrix (bright phase).

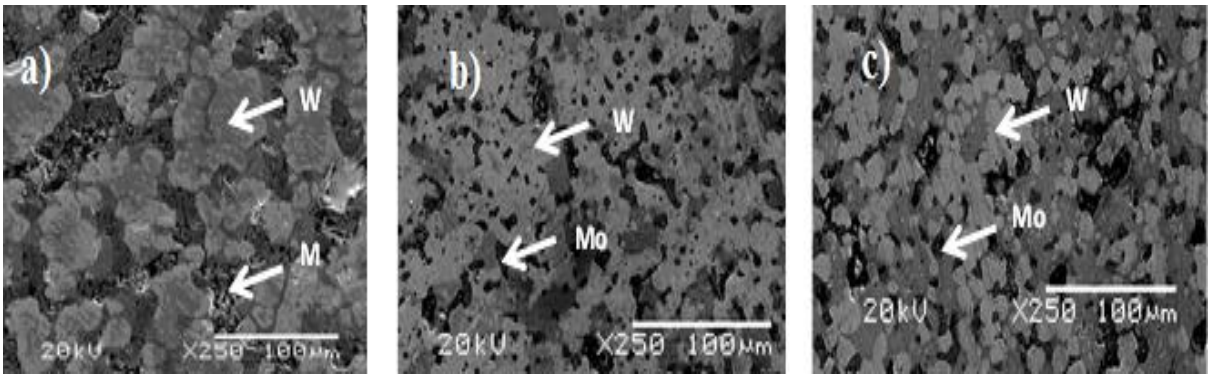

Fig. 5.2 SEM micrograph of a) Alloy A, b) Alloy B, c) Alloy C, milled for 20h and sintered at 1500°C for 2 h.

4.3 SINTEREBALITY STUDY

Fig. 6 shows the sintered density of compacted pellets of alloy (A through C) at different compaction pressure. The sintered density for all the alloys shows an increasing trend with an increase in compaction pressure. The results indicate that C alloy exhibits enhanced sinterability than the rest of the alloys. The sintering has been done at 1500°C in flowing Argon atmosphere at the rate of 100 ml per minute. The sinterability implies the efficiency in sintering, lesser number of pore implies better sinterability and vice versa. It has been found that green density is maximum at the pressure of 1000 MPa as compared to that of 500 and 750 MPa. The green densities of the compacted pellets have been evaluated by Archimedes's principle. In our experiment the alloy C shows better sinterability then the other alloys because with increase in Mo percentage the softening of material occur and reduction of size is higher so the compaction at the same atmosphere and pressure is much higher than the other two alloys.

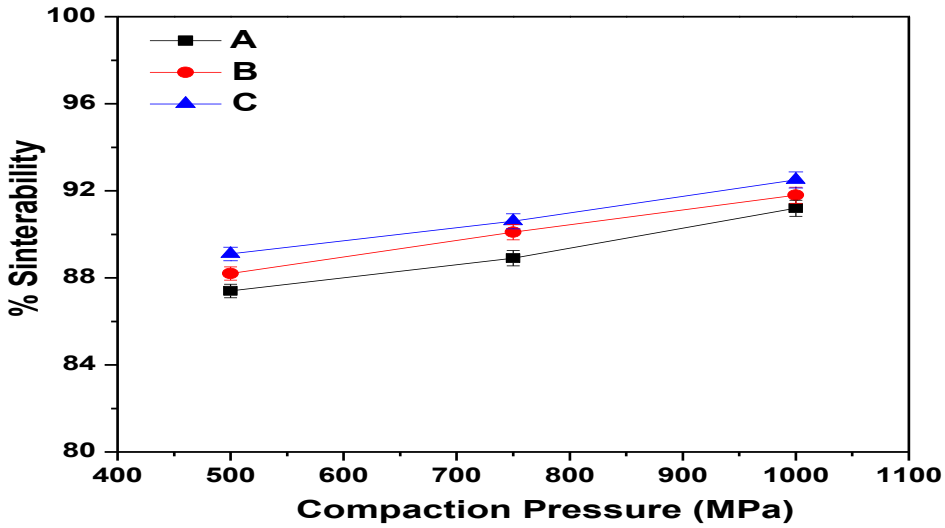

Fig. 6. Variation of sinterability for alloys A through C milled for 20h and sintered at 1500°C for 2 h.

4.4 HARDNESS STUDY

Fig. 7 shows the variation in hardness at different points along the cross-section of alloys A through C compacted at 1 GPa pressure and sintered at 1500°C for 2 h. The hardness of alloy A exhibits a lower value than the rest of the alloy along the contour. The hardness of alloy shows a lower value than the rest of the alloy. The alloy C shows the maximum hardness value because of the presence of high sintered density of the material in case of the alloy C as shown in case of the sinterability. The maximum hardness value shown by the alloys is

8.21GPa in case of alloy C and the alloys show the lowest value is 8.06 GPa in case of alloy A.

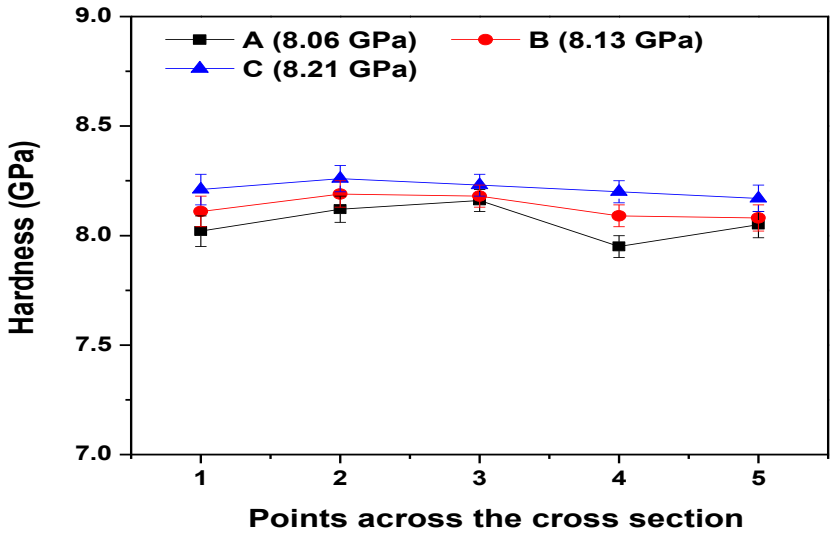

Fig.7. Variation of Hardness for alloys A through C milled for 20h and sintered at 1500°C for 2 h.

4.5 COMPRESSION STUDY

Fig. 8 shows actual stress true strain curve of the sintered samples of alloy A through C under compressive loading at room temperature. All the alloys show the similar kind of strain hardening behavior. It can be seen from the figure that alloy C shows maximum compressive strength whereas the alloy A shows the minimum value of compressive strength. The alloy C exhibit higher density and hardness as compared to rest of the alloys due to that the load carrying capacity is higher than the others. Both molybdenum and tungsten both are brittle in nature so there is not any gross plastic deformation take place in all three alloys.

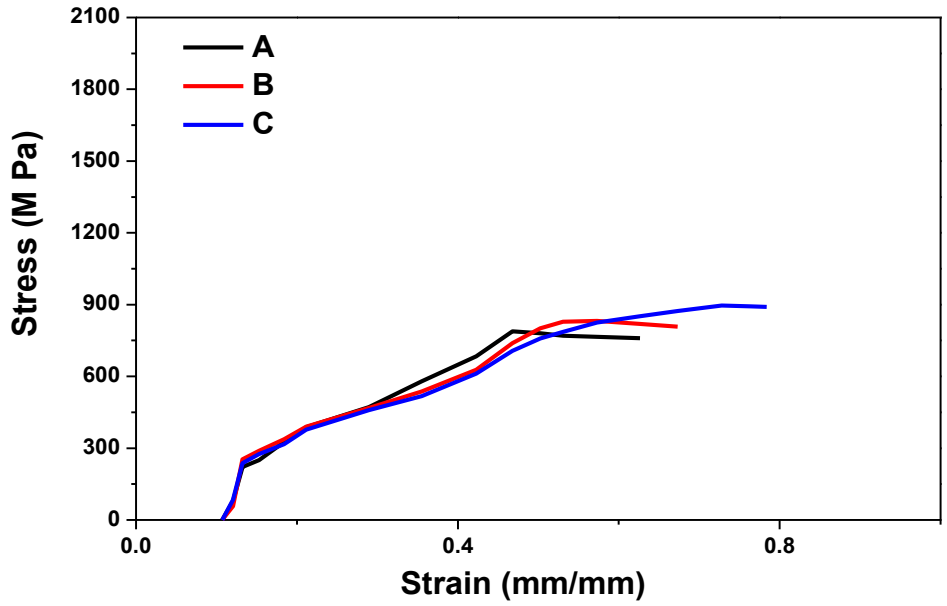

Fig. 8. Compressive stress strain curve of alloys A through C milled for 20h and sintered at 1500°C for 2 h.

4.6 WEAR STUDY

Fig. 9 displays the variation in wear depth with sliding distance traversed by the indenter on the sample surface for alloys A through C. It is evident that alloy C shows minimum wear depth than other alloys (A through C) for same traversed time and distance by the indenter. Wear test is conducted to gain the knowledge about the material in actual practice in the cyclic loading condition.

Here in case of wear test the applied load is 20 KN for 10min and the rotating speed is 25 rpm. The result shows that the wear depth in case of alloy C is minimum because of the low crystallite size and high strength of the alloy C. wear depth and sliding distance are the function of time.

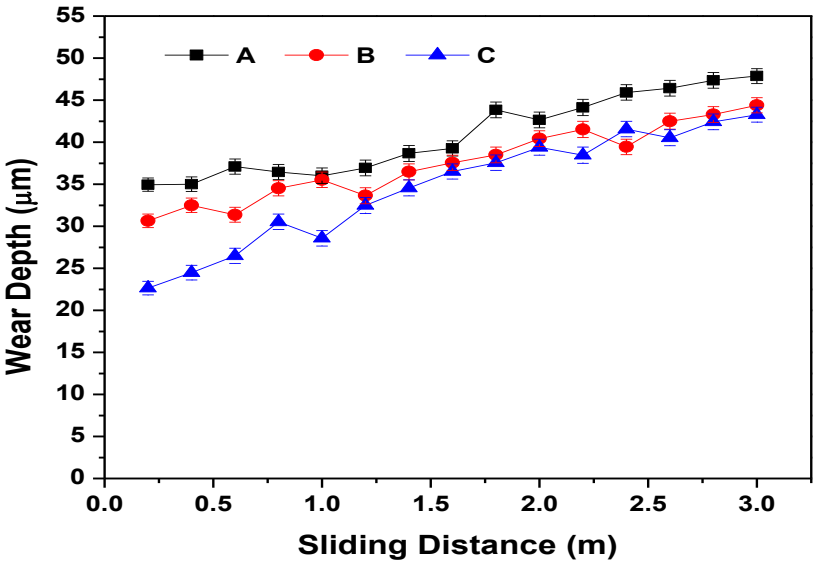

Fig. 9. Variation of Wear depth for alloys A through C milled for 20 h and sintered at 1500°C for 2 h.

4.7 OXIDATION STUDY

Fig. 10 displays the oxidation behavior of alloy A through C at 1000°C time periods up to 6 h. The results show rapid oxidation rate in case of alloy A to C. Initially rapid oxidation for alloys A to C is due to formation of porous oxide (WO_3) which increases the diffusion of oxygen as evident from Fig 11. The decrease in the rate of oxidation after a particular time is due to the formation of a more dense oxide (WO_2) than WO_3 which restrict the inward diffusion of oxygen.

Alloy C shows better oxidation resistance than alloy A and B due to the formation of a more stable oxide (W_5O_{14}) which shows more resistance to rupturing of film than WO_3. All the formation of oxides are confirmed by the XRD of the formed oxides. Which proves that alloy A and alloy B does not go for the formation of (W_5O_{14}) because of the lack of the Mo molecule in the case of these alloys.

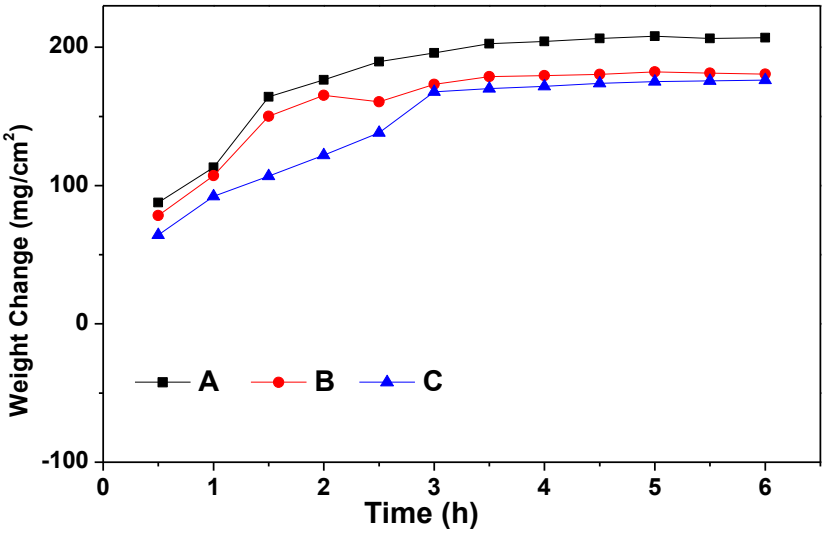

Fig. 10. Weight change as a function of exposure time for the oxidation of alloys A through C at 1000°C.

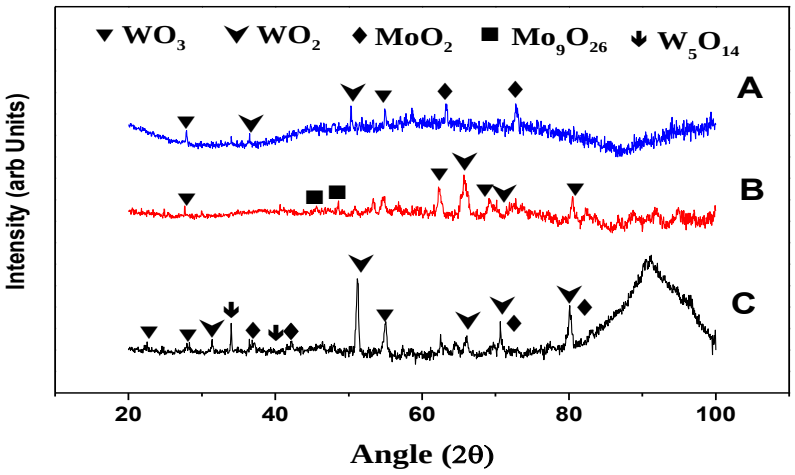

Fig. 11. XRD pattern of alloy A through C oxidized at 1000°C for 6 h.

Table 2. Shows comparative study of physical, mechanical properties of all the investigated alloys. It is evident from the table that Alloy C ($W_{50}Mo_{50}$) shows best physical, mechanical properties as compared to rest of the alloys.

Table 2: Comparative study of the investigated alloys

Parameters	$W_{90}Mo_{10}$	$W_{70}Mo_{30}$	$W_{50}Mo_{50}$
Crystallite Size (nm) (min)	38.7	37.8	34.7
Lattice strain (%) (max)	0.41	0.45	0.47
Dislocation Density ($10^{16}/m^2$) (max)	13.07	13.04	15.66
Sinterability (%) (Compaction pressure = 1 GPa, sintered at 1500°C for 2 h)	91.2	91.8	92.5
Hardness (GPa) (Compaction pressure = 1 GPa, sintered at 1500°C for 2 h)	8.06	8.13	8.21
Compressive strength (GPa) (max)	0.79	0.83	0.89

CONCLUSIONS

The following conclusions may be made from the present study:

1. The alloy C ($W_{50}Mo_{50}$) shows minimum crystallite size and maximum lattice strain and dislocation density due to presence of high percentage of molybdenum which causes more softening of the lattice to that of other alloys which results is higher percentage of size reduction.
2. The lattice parameter for all alloys shows an increasing trend at 10 h due to exertion of negative hydrostatic pressure by nano-crystals and decreasing trend at 20 h of milling due to formation of solid solution.

3. Maximum sintered density is achieved in alloy C, i.e, ($W_{50}Mo_{50}$).
4. Highest Compressive strength, hardness, sinterability, is shown by the alloy C ($W_{50}Mo_{50}$).

Overall we can say that the alloy C ($W_{50}Mo_{50}$) shows excellent property then the other two alloys.

SCOPES FOR FUTURE WORK

- Fabrication and characterization of W based alloys by advanced consolidation technique such as spark plasma sintering.
- Liquid phase sintering of W based alloys can be done by the addition of alloying element like Ni, which increases both mechanical and physical property of alloy.
- Study the deformation mechanism of W based alloy in compressive mode.
- Study the effect of multi-oxide dispersion on microstructure, mechanical and oxidation behavior in W based alloys.
- Addition of several oxide may increase the oxidation resistance and other mechanical properties, so oxides material like Y_2O_3, ZrO_2, La_2O_3 can be added to increase the property.

REFERENCES

[1] C. Suryanarayana, Prog. In Mat. Sci., 46 (2001) 1-184.

[2] C. Suryanarayana, Mechanical Alloying and Milling, Marcel Dekker Inc, New York, 2004, pp. 13.

[3] W. F. Smith, Structure and Properties of Engineering Alloys, Second Edition, McGraw-Hill, USA, 1993.

[4] Lassner E, Schubert W-D, Tungsten-properties, chemistry, technology of the element, alloys, and chemical compounds, Kluwer Academic/Plenum Publishers, New York, 1999, pp. 255-268.

[5] M. Trazaska, Intl. Jou, of Ref. Met. & Hard Mat., 14 (1996) 235.

[6] L. Uray, Intl. Jou, of Ref. Met. & Hard Mat., 20 (2002) 235.

[7] W. E. Gurwell, Materials & Manufacturing Processes., 9(6) (1994) 1115-1126.

[8] H. Hahn, J. Logas, R.S. Averbach, Jou. Of Mat.Research., 5 (1990) 609.

[9] C. C. Koch, Nanostruct Materials, 9 (1997) 13.

[10] H. Glieter, Nanostruct Mater, 6 (1995) 3.

[11] H. Glieter, Act. Mat., 48 (2001) 1.

[12] K. Lu, Materials Science & Engineering, R 16 (1996) 161-221.

[13] W. S. Wysong, Am. Inst. Mining Met. Engrs., 175 (1948) 611.

[14] W. W. Webb, J. T. Norton, C. Wagner, Jou of the Electrochem. Soc., 103 (1956) 2.

[15] J. W. Semmel, "High Temperature Materials", John Wiley & Sons, Inc., New York , (1959) 510-519.

[16] G. K. Williamson and W. H. Hall, Acta Met, 1 (1953) 22.

[17] G. K. Williamson and R. E. Smallman, Philos Mag, 1(1) (1956) 34–46.

[18] G. K. Williamson and R. E. Smallman, Philos Mag, 1(1) (1956) 34–46.

[19] R. E. Smallman, K. H. Westmacott, Philos Mag, 2(17) 1957, 669–683.

[20] Y. H. Zhao, H. W. Sheng, and K. Lu, Acta Met, 49 (2001) 365–375.

[21] Michael Robert Middlemas, ProQuest UMI Dissertations Publishing, DAI-B70/06 2009, 107-108.

[22] Suresh Telu, A. Patra , M. Sankaranarayana , R. Mitra , S. K. Pabi, Int. Jou of Refract Met and Hard Mater, 36 (2013) 192-194.

[23] Necati Ozkan & Brian J. Briscoe, J. Eur. Ceram. Soc. 14 (1994) 143-151.